

Synthesis of silver nanoparticles using curcumin-cyclodextrins loaded into bacterial cellulose based hydrogels for wound dressing applications

Item Type	Journal article
Authors	Gupta, Abhishek;Briffa, Sophie M;Swingler, Sam;Gibson, Hazel;Kannappan, Vinodh;Adamus, Grazyna;Kowalczyk, Marek M;Martin, Claire;Radecka, Iza
Citation	Gupta, A., Briffa, S. M., Swingler, S., Gibson, H., Kannappan, V., Adamus, G., Kowalczyk, M. M., Martin, C. and Radecka, I. (2020) Synthesis of silver nanoparticles using curcumin-cyclodextrins loaded into bacterial cellulose based hydrogels for wound dressing applications, <i>Biomacromolecules</i> , 21(5), pp. 1802–1811. https://doi.org/10.1021/acs.biomac.9b01724
DOI	10.1021/acs.biomac.9b01724
Publisher	American Chemical Society (ACS)
Journal	Biomacromolecules
Download date	2026-06-15 08:12:30
License	https://creativecommons.org/licenses/by-nc-nd/4.0/
Link to Item	http://hdl.handle.net/2436/623029

Synthesis of silver nanoparticles using curcumin-cyclodextrins loaded into bacterial cellulose based hydrogels for wound dressing applications

Abhishek Gupta^{1,4*}, Sophie M Briffa², Sam Swingler³, Hazel Gibson^{3,4}, Vinodh Kannappan⁴,
Grazyna Adamus⁵, Marek Kowalczyk^{5*}, Claire Martin⁶, Iza Radecka^{3,4*}

¹School of Pharmacy, Faculty of Science and Engineering, University of Wolverhampton, WV1 1LY Wolverhampton, UK

² School of Geography, Earth and Environmental Sciences, University of Birmingham, UK

³Wolverhampton School of Sciences, Faculty of Science and Engineering, University of Wolverhampton, WV1 1LY, Wolverhampton, UK

⁴Research Institute in Healthcare Science, Faculty of Science and Engineering, University of Wolverhampton, WV1 1LY Wolverhampton, UK

⁵Centre of Polymer and Carbon Materials, Polish Academy of Sciences, M. Curie-Skłodowskiej 34, 41-819 Zabrze, Poland

⁶Department of Biological Sciences, School of Sciences and the Environment, University of Worcester, UK

Keywords: silver nanoparticles, green chemistry, antimicrobial, hydrogel dressing, bacterial cellulose, curcumin reduced silver nanoparticles

ABSTRACT

Chronic wounds are often recalcitrant to treatment due to high microbial bioburden and the problem of microbial resistance. Silver is a broad spectrum natural antimicrobial agent with wide applications extending to proprietary wound dressings. Recently silver nanoparticles have attracted attention in wound management. In the current study, the green synthesis of nanoparticles was accomplished using a natural reducing agent, curcumin which is a natural polyphenolic compound, well known as a wound healing agent. The hydrophobicity of curcumin was overcome by its microencapsulation in cyclodextrins. This study demonstrates the production, characterisation of silver nanoparticles using aqueous curcumin:hydroxypropyl- β -cyclodextrin complex and loading them into bacterial cellulose hydrogel with moist wound healing properties. These silver nanoparticle-loaded bacterial cellulose hydrogels were characterised for wound management applications. In addition to high cytocompatibility, these novel dressings exhibited antimicrobial activity against three common wound infecting pathogenic microbes *Staphylococcus aureus*, *Pseudomonas. aeruginosa* and *Candida auris*.

▪ INTRODUCTION

Microbial colonisation, where is not wanted, can led to severe infections which can result in disability, disease and even death. Wound infections are one of the major factors resulting in impaired healing¹⁻³. Wounds colonised by opportunistic microbes may fail to follow the natural reparative and regenerative stages involved in healing process⁴. In addition uncontrolled infections can prevent the restoration of the anatomical and physiological integrity resulting in chronic non-healing wounds^{5,6}. To prevent infections, modern medicine is dependent on antimicrobial agents such as antibiotics which can either destroy pathogens or inhibit their growth. Unfortunately, the misuse of antibiotics has resulted in the emergence of a number of multiresistant microbes. Therefore antibiotic therapy often proves ineffective in eradicating infections in chronic non-healing wounds³. Owing to the site specific delivery, increased target site concentration, reduced adverse effects, use of agents not suitable for oral and systemic therapy and low incidence of resistance^{7,8}, antimicrobial-loaded wound dressings have attracted wide interest as a concurrent wound management regime.

Hydrogels are one of the promising candidates as wound dressings due to their unprecedented properties including their ability to maintain a moist microclimate at the wound site which is proven to facilitate healing⁹⁻¹¹. A number of natural and synthetic polymeric materials are in use to produce hydrogel dressings^{12,13}. Bacterial cellulose (BC) is an example of a natural biosynthetic cellulose hydrogel which due to its unique properties has been widely considered as a wound dressing¹⁴⁻¹⁸. BC can be produced by several bacteria but *Gluconacetobacter xylinus* (*G. xylinus*) is considered as one of the best for BC production¹⁹. Our group has previously reported the findings on the physicochemical characterisation and suitability of BC hydrogels as

1
2
3 wound dressings²⁰. Although BC does not have inherent antimicrobial activity however, its
4 cross-linked fibre network structure encouraged several research attempts of loading
5 antimicrobials, anti-inflammatory, antioxidants and other healing agents for wound dressing
6 applications^{17,21,22}. In continuation, in the presented study, an investigation has been made to
7 produce biosynthetic hydrogels with healing properties for chronic wound management. Our
8 novel approach is consistent with the concept of the forensic engineering of advanced polymeric
9 materials (FEAPM) which can help to understand the relationships between the structure of the
10 biomaterial used, its properties and behaviour for practical applications²³.
11
12
13
14
15
16
17
18
19
20
21

22 Currently the treatment of microbial infections is severely affected by the emergence of new
23 multiresistant microbes, including bacteria and fungi. Gram-positive *Staphylococcus aureus* has
24 a great ability to develop multiple drug resistances. Similarly, Gram negative *Pseudomonas*
25 *aeruginosa*, a common opportunistic pathogen shows resistance to most penicillins,
26 cephalosporins and carbapenems. Pathogenic fungi such as *Candida auris* pose a significant
27 health risk to patients suffering from infected wounds and in particular to immunocompromised
28 individuals which can result in candidiasis/candidemia and invasive aspergillosis. Recently a
29 new multidrug resistant strain of *C. auris* was discovered²⁴ and has quickly become a prolific
30 nosocomial pathogen in the UK^{25,26}, with diagnoses on all continents with 33 countries reporting
31 incidents of antifungal resistance. *C. auris* is resistant to most first and second-generation
32 antifungals with 90% of isolates being resistant to fluconazole, 40% resistant to amphotericin
33 and 2% to echinocandins such as caspofungin²⁷⁻²⁹. The concern regarding these pathogens
34 centres around the increasing resistance they are showing towards a very limited pool of
35 effective antimicrobials³⁰⁻³² and hence the focus is on targeted delivery by antimicrobial wound
36 dressings.
37
38
39
40
41
42
43
44
45
46
47
48
49
50
51
52
53
54
55
56
57
58
59
60

1
2
3 Silver is a well-known antimicrobial effective against fungi, yeast and bacteria including several
4 antibiotic resistance strains³³⁻³⁵. The emergence of nanotechnology enabling the production of
5 silver nanoparticles has served a new therapeutic modality. Silver nanoparticles (AgNP) owing
6 to their characteristic broad-spectrum antimicrobial properties have received increased focus in
7 biomedical applications including for wound management³⁶⁻³⁸. Among the several different
8 approaches to synthesise AgNP, the use of natural substances like plant extracts has received
9 wide research consideration due to the safe and eco-friendly procedure^{37,39-41}.

10
11
12 Curcumin (CUR), a natural polyphenol, extracted from turmeric is a well-known wound healing
13 agent with proven antimicrobial, antioxidant and anti-inflammatory effects^{22,42}. In addition to its
14 healing properties, CUR has been used as a reducing and capping agent to produce AgNP⁴³. The
15 main challenge that limits the wider biomedical application of CUR is its hydrophobic nature.
16 Several chemical mediators like dimethyl sulfoxide, dichloromethane, sodium carbonate are
17 employed in AgNP synthesis from CUR⁴⁴⁻⁴⁸. These chemical mediators can have serious
18 cytotoxic effects⁴⁸. Selection of solvent medium, reducing agent and nontoxic stabiliser are the
19 main considerations in green nanoparticle production^{49,50}. The current study reports the
20 production of AgNP following a green chemistry approach using an aqueous solution of
21 curcumin:hydroxypropyl- β -cyclodextrin (CUR:HP β CD). These AgNP produced using
22 CUR:HP β CD (cAgNP) were characterised and loaded in the biosynthetic BC hydrogels to
23 produce hydrogel dressings. To the best of our knowledge, the protocol presented herein to
24 produce cAgNP is novel and this is the first time the production of cAgNP-loaded BC has been
25 reported. This report presents the unique combination of silver nanoparticles with curcumin in
26 the biosynthetic BC to obtain the hydrogels for wound management applications. This study

1
2
3 investigates the inherent antimicrobial, antioxidant and cytocompatibility properties of these
4
5 novel hydrogel dressings.
6
7

8
9 **▪ MATERIALS AND METHODS**

10
11 **Materials:**

12
13 *Gluconoacetobacter xylinus* (ATCC 23770), *Pseudomonas aeruginosa* (NCIMB 8295)
14 and *Staphylococcus aureus* (NCIMB 6571) were obtained from the University of
15
16 Wolverhampton culture collection. *Candida auris* (NCF 8971) was obtained from the
17
18 Public Health England Culture Collection, Porton Down, UK. A stock culture of *P.*
19
20 *aeruginosa* and *S. aureus* were resuscitated at 37 °C on tryptone soy agar (TSA) (Sigma-
21
22 Aldrich, UK), *G. xylinus* at 30 °C on mannitol agar and *C. auris* at 37 °C on Sabouraud
23
24 Dextrose Agar (SDA). HS media was prepared following the standard protocol⁵¹.
25
26 Material for mannitol agar, SDA and HS media were purchased from Lab M (UK).
27
28 Tryptone soya broth (TSB), disodium phosphate and citric acid were purchased from
29
30 Sigma-Aldrich (UK). Overnight broth cultures were prepared in appropriate medium
31
32 using the stock plates.
33
34
35
36
37
38
39
40

41 U251MG (U251), MSTO and Panc 1 cell lines were purchased from ATCC (UK).
42
43 Defibrinated horse whole blood was purchased from TCS Biosciences Ltd.
44
45
46
47

48 Silver nitrate was purchased from Fischer Scientific (UK). Hydroxypropyl- β -cyclodextrin
49
50 (parenteral grade) was kindly provided by Roquette (France). Curcumin and Dimethyl
51
52 sulfoxide (DMSO) (spectrophotometric grade) were purchased from Alfa Aesar (UK).
53
54 Ringer tablets were purchased from Lab M (UK). Thiazolyl Blue Tetrazolium Bromide
55
56
57
58
59
60

1
2
3 (MTT), sodium bicarbonate and 2,2-diphenyl-1-picrylhydrazyl (DPPH) were purchased
4 from Sigma-Aldrich (UK). Sodium chloride 0.9 % (w/v) (normal saline, intravenous
5 infusion) was purchased from Baxter, UK. Sodium hydroxide was purchased from Acros
6 Organics (UK). NaCl (5.8 g/L) and glycine (7.6 g/L) for preparing Sorensen's glycine
7 buffer were purchased from Sigma-Aldrich, UK. Trypsin was purchased from Lonza
8 (Belgium). Dulbecco's Modified Eagle's Medium (DMEM), Fetal Bovine Serum (FBS),
9 L-Glutamine and Antibiotic Antimycotic were purchased from Gibco (UK).

20 21 **Preparation of CUR:HP β CD inclusion complex:**

22
23
24 Inclusion complex was synthesised by the solvent evaporation method following the
25 protocol previously reported²². Briefly, CUR solution (0.79 g in 37.5 mL acetone) was
26 added dropwise to the aqueous HP β CD solution (3.0 g in 12.5 mL deionised water) under
27 constant stirring at room temperature for slow and complete evaporation of acetone. The
28 sample was centrifuged and the aqueous supernatant containing CUR:HP β CD inclusion
29 complex was frozen after filtration and lyophilised.
30
31
32
33
34
35
36
37
38
39

40 41 **Preparation and characterisation of cAgNP:**

42 43 **Preparation of cAgNP using CUR:HP β CD**

44
45 A novel green chemistry approach was developed for cAgNP synthesis by reducing silver
46 nitrate (AgNO₃) with aqueous solution of CUR:HP β CD. CUR:HP β CD (0.19 g) solution
47 was prepared by dissolving in deionised water (18 ml). CUR:HP β CD aqueous solution
48 was added drop-wise with constant stirring to 1 mM AgNO₃ aqueous solution (42 ml)
49 under boiling condition in a conical flasks. The mixed solutions were boiled for 3 h for
50
51
52
53
54
55
56
57
58
59
60

1
2
3 reduction of Ag ions followed by cooling at room temperature for 30 minutes. The flask
4 was covered with aluminium foil to maintain dark conditions throughout the reduction
5 process to avoid any photochemical reactions.
6
7
8
9

10 11 12 **Characterisation of cAgNP:**

13 14 **Dynamic Light Scattering (DLS) and Zeta potential**

15 DLS measurements were performed on a Malvern Zetasizer (nano ZS) at the University
16 of Birmingham. Five consecutive measurements were carried out at 25 °C with samples
17 equilibrated for 2 minutes before the measurements were started. The results were
18 averaged to calculate the mean size. The same instrument was used to obtain the Zeta
19 Potential values. The same samples were used for size measurements, equilibrated for 2
20 minutes before measurements were started. The results were obtained at 25 °C. Five
21 consecutive measurements were taken and averaged to calculate the zeta potential.
22
23
24
25
26
27
28
29
30
31
32
33
34

35 **Transmission Electron Microscopy (TEM)**

36 The shape, size and distribution of cAgNP produced using CUR:HP β CD was investigated
37 by TEM. Briefly, a drop of aqueous colloidal cAgNP was casted on a carbon-coated 300
38 mesh copper grid (agar scientific), left for 30 minutes, rinsed off and allowed to dry at
39 room temperature in a covered container. TEM imaging was performed using JEOL 1400
40 electron microscope, operated at 80 keV. Images were captured at different range of
41 magnifications. A 100 cAgNP were randomly selected and measured using ImageJ to
42 obtain the size distribution.
43
44
45
46
47
48
49
50
51
52
53
54
55
56
57
58
59
60

Preparation of cAgNP-loaded BC hydrogels

Production of bacterial cellulose hydrogels

Bacterial cellulose (BC) hydrogels were prepared by the protocol reported previously²². Briefly, *G. xylinus* was selected for BC production and hydrogels were biosynthesised in sterilised Hestrin and Schramm (HS) culture medium under static condition. BC pellicles were purified prior to experimental use.

Loading cAgNP in BC hydrogels

BC pellicles after purification were padded dry on sterilised filter paper and aseptically loaded with cAgNP by immersing in aqueous colloidal cAgNP overnight under agitated conditions at 4 °C.

Characterisation studies:

Morphological study by Scanning electron microscopy (SEM):

Morphology of BC (neat) has been previously reported^{22,52}. BC before purification, purified BC (neat) and cAgNP-loaded BC hydrogels were cut in to discs (8 mm) using a biopsy punch and lyophilised. These discs were then coated with ultrafine gold coating using SC500 fine coater (Emscope, Kent, UK) and placed on a carbon stub. The morphology of the samples was studied using Zeiss Evo 50 EP, SEM (Carl Zeiss AG, Oberkochen, Germany).

Energy dispersive X-ray (EDX) analysis:

Lyophilised cAgNP-loaded BC hydrogel samples were analysed by EDX (Zeiss Evo 50 EP, SEM) coupled with X-Max^N 50 Silicon Drift Detector (Oxford Instruments) and the analysis was performed by Oxford Instruments INCA Energy Dispersive Spectroscopy Nanoanalysis software using the Point & ID function, to confirm the presence of silver.

Moisture content (M_c)

The wet mass (W_w) of BC (neat) and cAgNP-loaded BC (test) hydrogels was recorded before lyophilisation and the dry mass (W_d) was measured after 72 h lyophilisation. M_c (%) was calculated using a formula:

$$\% M_c = \frac{(W_w - W_d)}{W_w} \times 100$$

Cytocompatibility study (*in vitro* cell viability):

Cytocompatibility of BC (neat) has been previously tested and reported using conditioned media²⁰ and BC discs²² on different mammalian cell lines. To study the cytocompatibility of cAgNP-loaded BC, *in vitro* cell viability test was performed using Panc 1 (human pancreatic ductal adenocarcinoma), U251 (human glioblastoma) and MSTO (human mesothelioma) following the protocol previously reported²².

All cell lines were cultured in Dulbecco's Modified Eagle's Medium (DMEM), supplemented with fetal bovine serum (FBS), Antibiotic Antimycotic and L-Glutamine at

1
2
3 37 °C in humidity incubator with 5 % CO₂. BC pellicles after pad drying were either
4 rehydrated with PBS (control) or cAgNP (test) overnight under agitated conditions (150
5 rpm) at 4 °C. These samples (control and test) were then aseptically cut in discs (8 mm)
6 using a biopsy punch for experimental purposes and temperature adjusted to 37 °C before
7 use.
8
9

10
11
12
13
14
15
16
17 Briefly, 25,000 cells were seeded per well (24 well plate) for 24 h at 37 °C in 5 % CO₂
18 incubator. The cells were exposed to either free cAgNP (equivalent amount) or cAgNP-
19 loaded BC (8 mm discs) for 24 h to investigate the effect on cell viability. Cells without
20 BC discs and PBS-loaded BC discs (8 mm) were used as controls respectively. Cell
21 viability was evaluated following the standard MTT assay previously reported²². Data
22 recorded was analysed statistically by two-way analysis of variance (ANOVA) with a
23 Tukey's multi comparisons test using GraphPad Prism.
24
25
26
27
28
29
30
31
32
33

34 35 **Haemocompatibility**

36
37 The haemocompatibility of cAgNP-loaded BC hydrogels was tested following the
38 protocol previously reported²². Briefly, defibrinated horse whole blood was washed twice
39 using commercially available normal saline (pH 5.5) and blood cells were re-suspended
40 in normal saline. cAgNP-loaded BC discs (8 mm) were cut using a biopsy punch and
41 incubated with 1.9 ml horse blood cells suspended in normal saline in test Eppendorf
42 tubes. The positive (+ve) control was blood cells suspended in distilled water and
43 negative (-ve) control was blood cells in normal saline. All the test and control Eppendorf
44 tubes were incubated at 4 °C for 2 h with periodic inversion (every 15 min). Post-
45
46
47
48
49
50
51
52
53
54
55
56
57
58
59
60

1
2
3 incubation, after the removal of BC discs from test Eppendorf tubes, all the tubes were
4
5 centrifuged at 3000 rpm for 10 min at 4 °C. The supernatant was decanted and absorbance
6
7 was recorded (540 nm) to calculate percentage haemolysis (% Haemolysis).
8
9

10
11
12
13
$$\% \text{ Haemolysis} = \frac{(\text{Abs of sample}) - (\text{Abs of - ve control})}{(\text{Abs of + ve control}) - (\text{Abs of - ve control})} \times 100$$

14
15
16
17
18
19
20
21
22

23 **Antimicrobial study (Disc diffusion assay)**

24
25 The antimicrobial activity of cAgNP-loaded BC was investigated against *P. aeruginosa*
26
27 (Gram -ve), *S. aureus* (Gram +ve) bacteria and *C. auris* using the disc diffusion assay.
28
29 PBS-loaded BC and HPβCD-loaded BC were used as controls. Discs (8 mm) of PBS-
30
31 loaded BC, HPβCD-loaded BC and cAgNP-loaded BC were placed aseptically on TSA
32
33 plates spread with an overnight culture of *P. aeruginosa* or *S. aureus* and SDA plates
34
35 were spread with an overnight culture of *C. auris* and incubated at 37 °C for 24 h and
36
37 zone of inhibition (ZOI) were measured. Data is presented as mean ± standard deviation
38
39 (SD) and analysed statistically by two-way ANOVA with a Tukey's multi comparisons
40
41 test using GraphPad Prism.
42
43
44
45
46
47

48 **Anti-oxidant study by DPPH assay**

49
50 The antioxidant potential of cAgNP produced using CUR:HPβCD was evaluated using
51
52 2,2-diphenyl-1-picrylhydrazyl (DPPH) radical scavenging assay. The assay mixture with
53
54 1 ml DPPH (80 µg/mL) methanolic solution and 1 ml of test colloidal cAgNP (including
55
56
57
58
59
60

1
2
3 the blank) after mixing were incubated for 30 min in dark at the room temperature.
4
5 Absorbance was recorded (517 nm) and the free radical scavenging potential was
6
7 calculated as percent antioxidant effect (% E) as:
8
9

$$\% E = \frac{Abs_{control} - Abs_{sample}}{Abs_{control}} \times 100$$

20 21 **Transparency test**

22
23 Monitoring the healing process without the need of removing dressing could help
24
25 minimise trauma to the granulating tissue. With the aim of wound dressing application,
26
27 the transparency level of cAgNP-loaded BC hydrogels was assessed by simulation. PBS-
28
29 loaded BC and cAgNP-loaded-BC hydrogels were transferred on the laminated sheet of
30
31 paper with text typed in different colours. The clarity of text underneath the hydrogel was
32
33 examined to determine if the healing tissue at the wound site could be observed through
34
35 these hydrogels.
36
37
38
39
40
41
42
43
44
45
46
47
48
49
50
51
52
53
54
55
56
57
58
59
60

■ RESULTS AND DISCUSSION

Preparation of cAgNP and cAgNP-loaded BC hydrogels

Most of the AgNP synthesis methods involve the use of organic solvents and toxic reducing agents with the potential threat to the environment and cytotoxic effect on mammalian cell lines. The method reported herein involved bio-reduction of AgNO₃ with an aqueous suspension of CUR:HPβCD resulting in nanoparticle formation. The colour changed from colourless to pale yellow at the start of CUR:HPβCD addition which intensified with increased dosage and subsequently changed to yellow-brown with time, suggesting the production of nanoparticles. This could be due to the excitation of surface plasmon vibrations in AgNPs, which is in accordance with literature^{40,53}.

G. xylinus produced BC hydrogel pellicles which were harvested and purified. BC pellicles became clear after purification. These results are in accordance with previous reports^{15,22,33,52,54}. When the purified padded dry BC was rehydrated with the aqueous colloidal cAgNP, the pellicles re-swelled and the colour changed to yellow-brown. These cAgNP-loaded BC hydrogels were stored at 4 °C throughout the experimental procedure.

Characterisation of cAgNP and cAgNP-loaded BC hydrogels

The formation of colloidal cAgNP produced was confirmed by testing its properties like size distribution and charge. After loading aqueous colloidal cAgNP in the padded dry BC, the physicochemical and *in vitro* haemocompatibility and cytocompatibility hydrogels were investigated.

Particle size distribution and surface charge by TEM, DLS and zeta potential

The size and morphology of cAgNP produced using CUR:HP β CD were studied from the TEM images (Fig.1a-c). TEM imaging showed that the morphology of the nanoparticles was mainly spherical in shape with smooth edges. The majority of bio-reduced cAgNP were in the diameter range of 20-55 nm (80 %) and the average size of 42.71 ± 17.97 nm. (Fig.1a-c). It emerged from the results that nanoparticles were homogeneously surrounded by a thin layer of capping material. As the method employed in the current work only involved AgNO₃ and CUR:HP β CD, without the use of any organic solvents and additional capping agents, this suggests that CUR:HP β CD was acting both as a reducing and capping agent. These results are in agreement with literature reporting the use of curcumin as a reducing and capping agent^{40,43,46,48,53}.

DLS measurements identified nanoparticles with the hydrodynamic diameter in the range of 182.10 ± 8.83 nm (Fig 1d) and the Poly dispersity index (PDI) value of 0.196 ± 0.009 . These results indicate both, the nucleation to form new nanoparticles and aggregation could be happening consecutively. These findings are consistent with studies reported in literature^{53,55}. Low PDI indicating that the colloidal cAgNP was not very polydispersed.

The zeta potential value is directly proportional to the stability of nanoparticle dispersion⁵⁵. Zeta potential studies revealed a negative charge on the synthesised nanoparticles with the magnitude of -20.1 ± 0.702 mV. These findings are in a close range to the previously reported values for AgNP bio-reduced using curcumin⁴³.

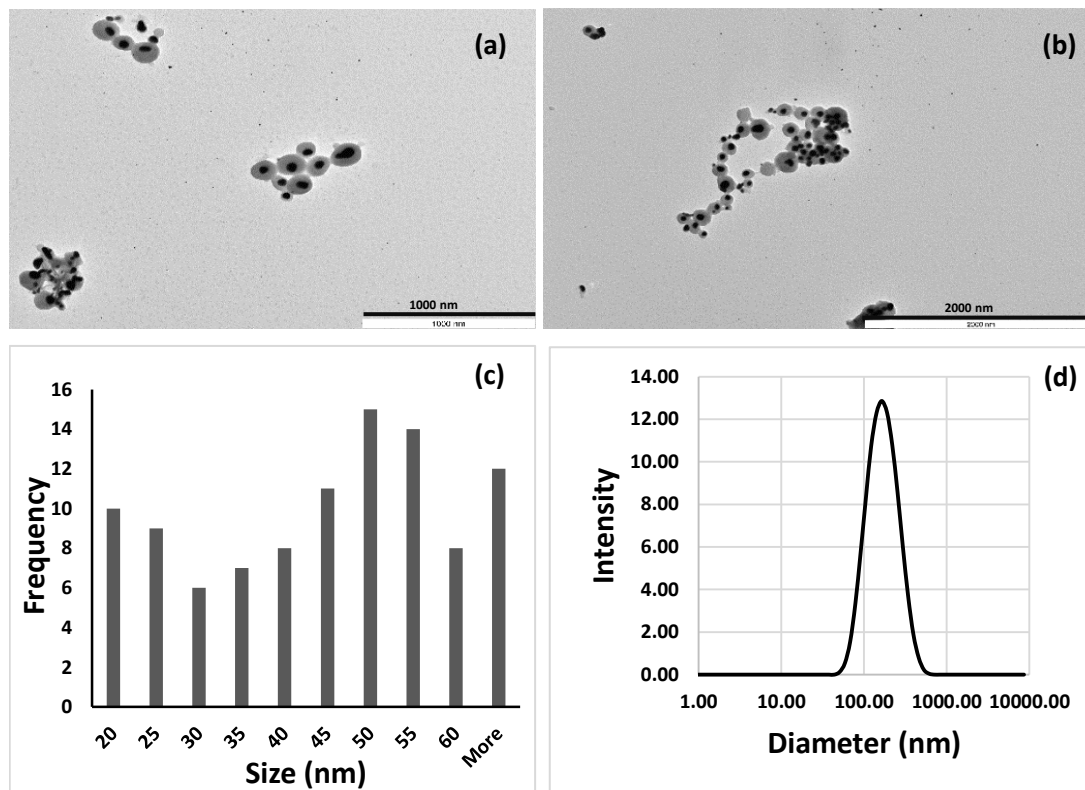


Figure 1. Characterisation of cAgNP produced using CUR:HP β CD, (a-b) TEM photomicrographs (c) size distribution as measured by TEM analysis and calculated with 100 nanoparticles (d) DLS data of cAgNP with size distribution.

Scanning electron microscopy (SEM)

BC has a fine fibre network structure with voids^{21,22,52}. SEM images revealed *G. xylinus* trapped in the cellulose network before purification (Fig 2a) and bacteria were successfully removed on purification (Fig 2b). The interspersed voids in the interwoven cellulose ribbons of BC allow impregnation of healing agents^{17,33,56}. SEM of lyophilised cAgNP-loaded BC revealed that cAgNP penetrated through the voids during rehydration of padded dry BC pellicles and got physically trapped in the fibre network structure (Fig 2c). Also, it emerged that along with bio-reduced cAgNP, there was free CUR:HP β CD trapped in the BC. In addition to the reducing and capping properties in cAgNP synthesis, CUR:HP β CD has been demonstrated to have wound healing properties²². The excess of CUR inclusion complex in cAgNP-loaded BC may deliver additional benefits contributing to wound healing.

Morphology and size of nanoparticles was also determined in the SEM photomicrographs (Fig 2d). The average diameter was in the range of 37.2 - 65.1 nm and most of the nanoparticles appeared spherical. These results are in accordance with TEM results discussed in section above.

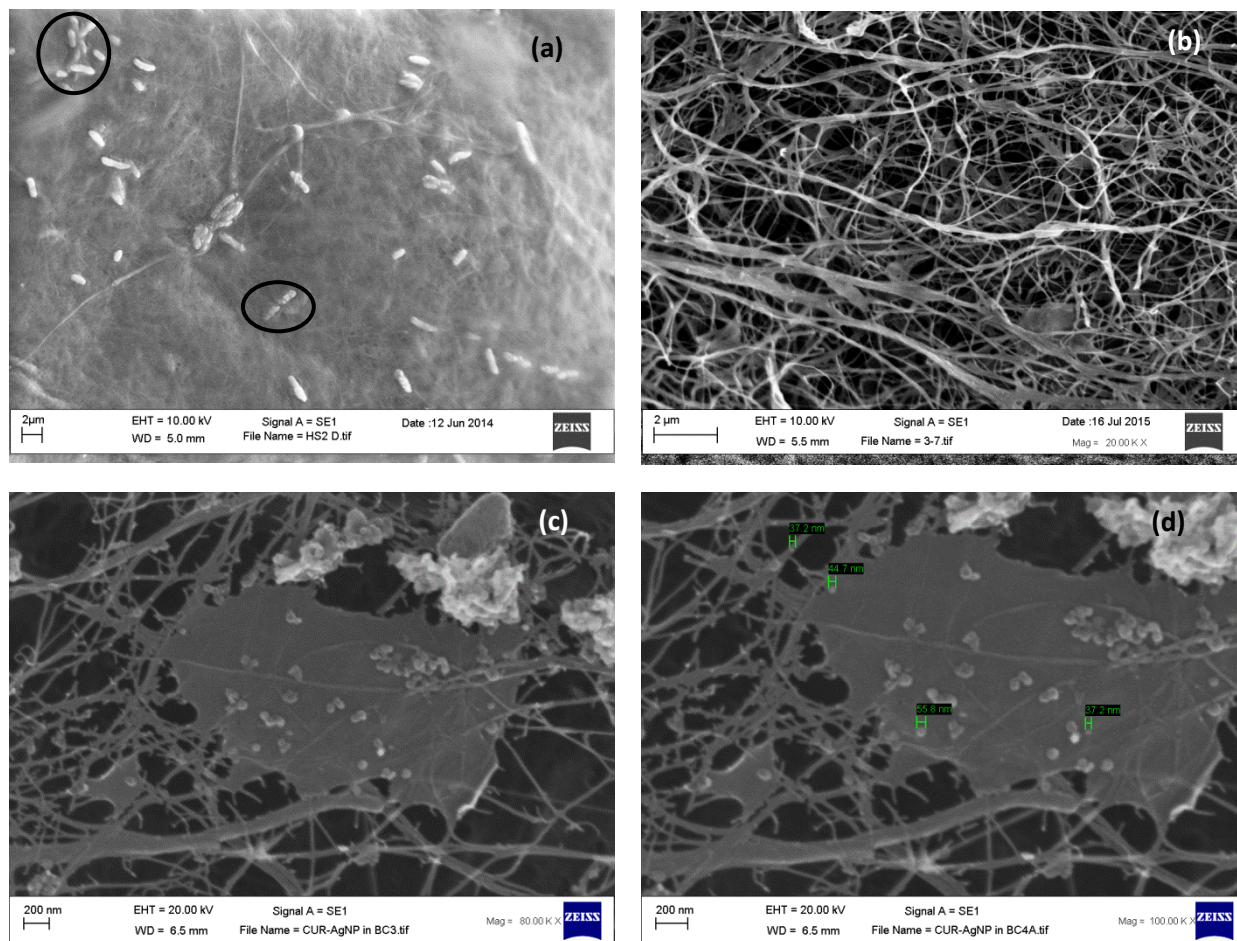


Figure 2. SEM photomicrographs of (a) Unwashed BC, entangled *G. xylinus* highlighted, (b) BC after purification, (c) & (d) cAgNP loaded in BC fibre network.

Energy dispersive X-ray (EDX) analysis

The elemental analysis was carried out by EDX studies. The results confirmed that BC (neat) is composed mainly of carbon and oxygen which is in accordance with our previously reported data³³. In addition to carbon and oxygen, detection of silver in the EDX spectra of cAgNP-loaded BC (test) confirmed nanoparticle loading in the test samples (Fig. 3).

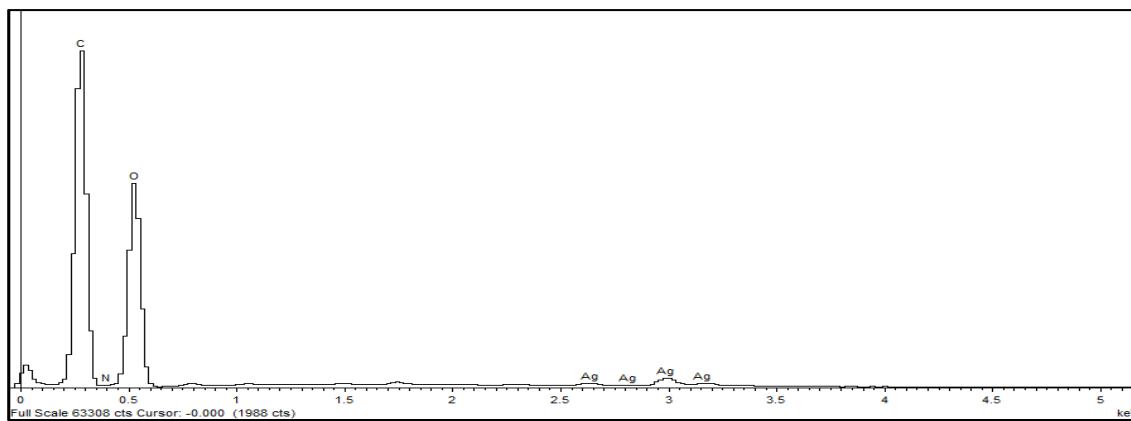


Figure 3. EDX spectrum of cAgNP-loaded BC.

Moisture content (M_c)

BC hydrogels have been reported to have a unique property of resistance to degradation despite considerable moisture content which is several times its dry mass¹⁴. This strength is contributed by its cross-linked fibre network structure. In the current study, the moisture content of neat BC and cAgNP-loaded BC hydrogels was evaluated. The results confirmed that neat BC pellicles imbibed 99.68 ± 0.09 % (v/w) ($n = 3$) water which is in accordance with previously reported data (> 99.5 %) for neat BC hydrogels^{20,22}. Moreover, the study on cAgNP-loaded BC revealed that the moisture content in these hydrogels was 98.86 ± 0.04 % ($n = 3$). These findings indicate that the difference in the

1
2
3 mass of neat BC and cAgNP-loaded BC is contributed by cAgNP and CUR:HP β CD that
4 gets physically trapped in the fibre network of BC during the loading process.
5
6
7
8
9

10 The high moisture content in BC can confer many benefits such as increased malleability,
11 soft texture and creating a moist environment with increased dissolved oxygen to
12 facilitate aerobic conditions at the wound-dressing interface. In addition, these hydrogels
13 may ease removal of the dressing, reduce pain sensation and therefore improve patient
14 comfort. These features have been reported to facilitate the wound healing
15 process^{15,21,57,58} and therefore BC has attracted increased interest in the wound care
16 sector.
17
18
19
20
21
22
23
24
25
26
27

28 **Cytocompatibility (*In vitro* study)**

29
30
31 Cytocompatible nature of BC is well documented in literature^{20,21,22,59}. It is one of the
32 many intrinsic features that resulted in BC based proprietary products like DermafillTM,
33 Biofill[®], XCell[®], and Gengiflex[®]^{57,60-62}. In this study, the cytocompatibility of cAgNP-
34 loaded BC hydrogels was evaluated using three different mammalian cell lines. The
35 cytotoxicity as determined by MTT assay revealed that cAgNP-loaded BC is
36 cytocompatible as all the tested cell lines demonstrated good survival rate (Fig. 4a).
37
38
39
40
41
42
43
44
45
46
47

48 Furthermore, we compared the cytocompatibility of free cAgNP to cAgNP-loaded BC on
49 U251, MSTO and Panc 1 cell lines. The results demonstrated that free cAgNP had
50 cytotoxic effect on all the tested cell lines resulting in lower cell viability compared to
51 cAgNP-loaded in BC ($p < 0.001$) (Fig. 4 a,b). These results suggest that BC controls the
52
53
54
55
56
57
58
59
60

1
2
3 release of cAgNP thus minimising the cytotoxic effect on the mammalian cells. These
4
5 findings support the potential application of cAgNP-loaded BC for wound management
6
7 as hydrogel dressings.
8
9
10
11
12
13
14
15
16
17
18
19
20
21
22
23
24
25
26
27
28
29
30
31
32
33
34
35
36
37
38
39
40
41
42
43
44
45
46
47
48
49
50
51
52
53
54
55
56
57
58
59
60

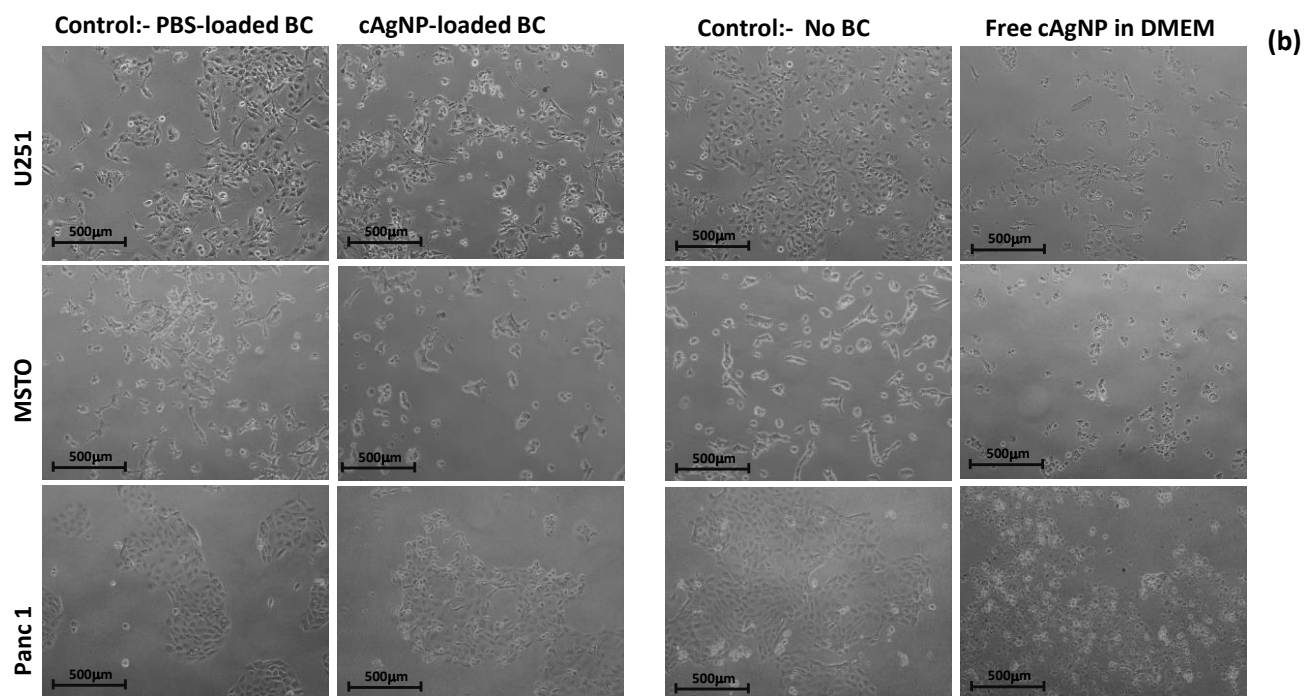
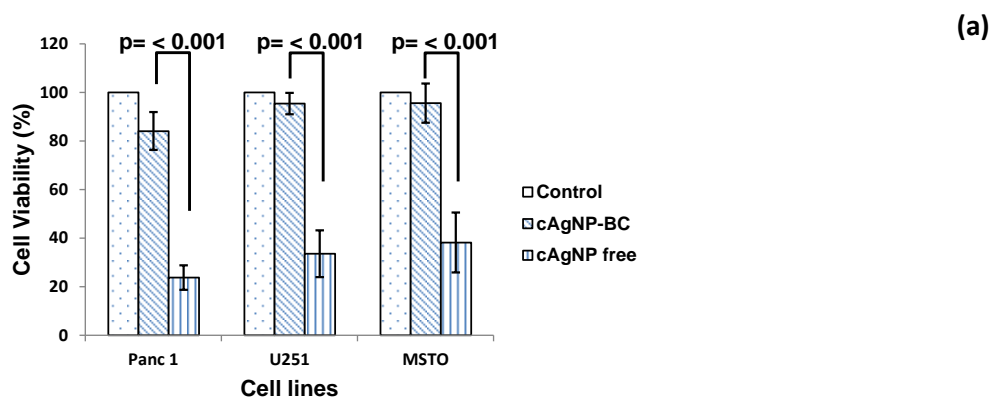


Figure 4. Cytocompatibility test results. (a) Bar graph showing the cell viability (%) after 24 h exposure to cAgNP-loaded BC and free cAgNP (equivalent amount) ($n = 8$). Representative photomicrographs of cells (10x magnification) after exposure to cAgNP-loaded BC and free cAgNP for 24 h.

Haemocompatibility

Haemocompatibility is an important property for biomedical applications of a material. BC has been reported to be haemocompatible hence it has been used in proprietary wound dressings^{20,63,64}. In the current study, cAgNPs were prepared in deionised water hence the hypothesis was drawn that cAgNP-loaded BC hydrogels may have haemolytic properties. The test results revealed that cAgNP-loaded BC hydrogels have a percentage haemolysis of 6.85 ± 1.12 % (n = 6). According to the ASTM F756 standards haemolytic indices this range is over the threshold value of 5 % hence cAgNP-loaded BC hydrogels would be classified as a haemolytic material⁶⁵. The higher haemolysis (%) of the tested hydrogels could be attributed to the use of deionised water instead of the isotonic solution for the synthesis of cAgNP.

In the case of chronic wound, there could be necrotic tissue or slough at the wound bed hence the haemolytic behaviour of these hydrogels may be minimal. Further research on the production of AgNP using CUR:HP β CD dissolved in isotonic solution may improve haemocompatibility of these hydrogels.

Antimicrobial study

Invasion of opportunistic microbes could impair wound healing leading to chronic non-healing wounds^{6,66}. Silver nanoparticles have been intensively studied as antimicrobial agents^{40,49,53}. Different mechanisms of action of AgNPs have been proposed as their antibacterial and antifungal effect is not completely known⁶⁷. In bacteria AgNPs have the ability to increase the permeability of cell membrane, interfere with DNA replication,

1
2
3 denaturation of bacterial proteins and release of silver ions inside the bacterial cell^{49,67}.
4
5 The antifungal action of silver nanoparticles are thought to increase the reactive oxygen
6
7 species within the fungal cell and increase membrane permeability resulting in cell
8
9 death⁶⁸.
10
11
12
13

14 In the current study, PBS-loaded BC, HP β CD-loaded BC and cAgNP-loaded BC
15
16 hydrogels were tested against *P. aeruginosa*, *S. aureus* and *C. auris* using the disc
17
18 diffusion assay at 24 h. PBS-loaded BC and HP β CD-loaded BC did not exhibit
19
20 antimicrobial activity however, cAgNP-loaded BC demonstrated significant antimicrobial
21
22 activity (p <0.001) against all three of the tested microbial strains (Fig. 5).
23
24
25
26
27

28 These results confirm the broad spectrum antimicrobial activity of cAgNP-loaded in BC.
29
30 Moreover, it immersed that cAgNP-loaded BC have stronger antimicrobial activity (Fig
31
32 5) against *P. aeruginosa* as compared to *S. aureus* (p < 0.001). This could be explained
33
34 by the difference in the cell structure of Gram positive and Gram negative bacteria.
35
36 AgNPs have been reported to have the ability to separate cytoplasm from bacterial cell
37
38 wall (plasmolysis effect) leading to the cell death in *P. aeruginosa*. In *S. aureus*, AgNPs
39
40 act differently and cause the bacterial cell death by inhibiting the cell wall
41
42 synthesis^{49,67,69}.
43
44
45
46
47
48
49
50
51
52
53
54
55
56
57
58
59
60

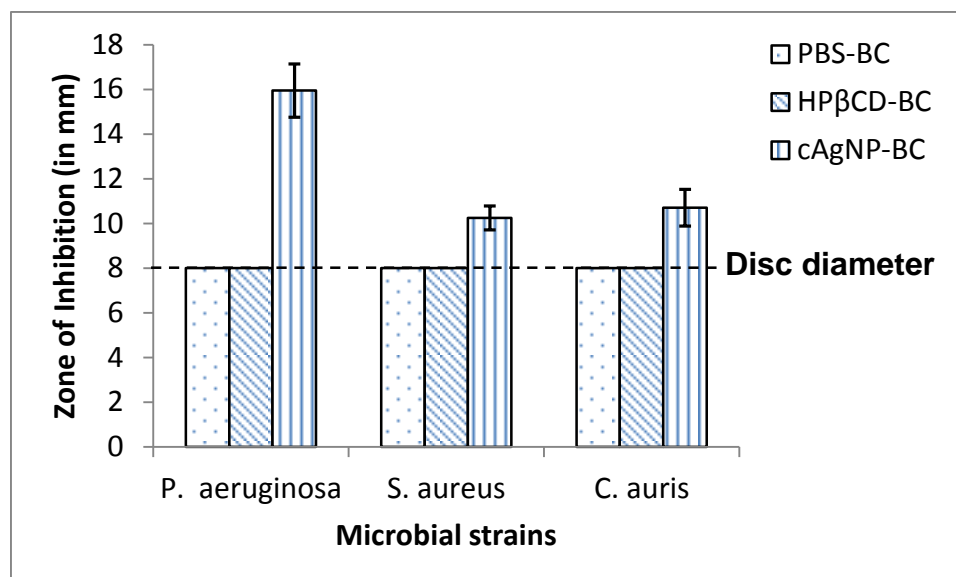


Figure 5. Antimicrobial disc diffusion assay results for PBS-loaded BC, HPβCD-loaded BC and cAgNP-loaded BC against *P. aeruginosa*, *S. aureus* and *C. auris* at 24 h (n = 10; error bars = SD).

Anti-oxidant activity of cAgNP by DPPH assay

Oxidative stress at the wound site may interfere with the healing process⁷⁰ hence a wound dressing with antioxidant properties along with antimicrobial activity may prove beneficial⁷¹. CUR has been reported to have healing properties including antimicrobial and antioxidant activities. It has been previously demonstrated that these properties were preserved in the inclusion complex of CUR in HPβCD²².

In the current study, cAgNP were successfully prepared using CUR:HPβCD as reducing and stabilising agent. The percent antioxidant effect (% E) for aqueous cAgNP colloidal suspension against DPPH was determined to be 76.65 ± 3.21 % (n = 6). The test results confirmed that silver nitrate and HPβCD does not have antioxidant activity which is in

1
2
3 accordance with previously reported findings²². These results confirmed that colloidal
4 cAgNP aqueous medium produced using CUR:HP β CD has antioxidant activity and when
5
6 loaded in BC to produce hydrogels, could prove beneficial in wound healing process.
7
8
9

10 11 12 13 14 **Transparency test**

15
16
17 Monitoring of wound healing process is vital from a clinical perspective⁷²⁻⁷⁴. Routinely,
18 this involves the removal of a dressing which can disturb the granulating tissue and could
19 cause trauma to the wound. A dressing with the feature enabling non-invasive monitoring
20 could be beneficial in wound healing.
21
22
23
24
25

26
27 The transparent nature of BC has already been reported²² and in this study, PBS-loaded
28 BC hydrogels reconfirmed these findings (Fig 6a). In this study, the transparency
29 property of cAgNP-loaded BC was evaluated by reading the text in different colours on
30 white laminated paper sheet through the test hydrogels. The results (Fig. 6b) demonstrate
31 cAgNP-loaded BC hydrogels allow monitoring the wound without the need for removal
32 of the dressing. This transparency testing is a simulation study and in order to confirm the
33 results, clinical validation would be required and could be evaluated using *in vivo* animal
34 models.
35
36
37
38
39
40
41
42
43
44
45
46
47
48
49
50
51
52
53
54
55
56
57
58
59
60

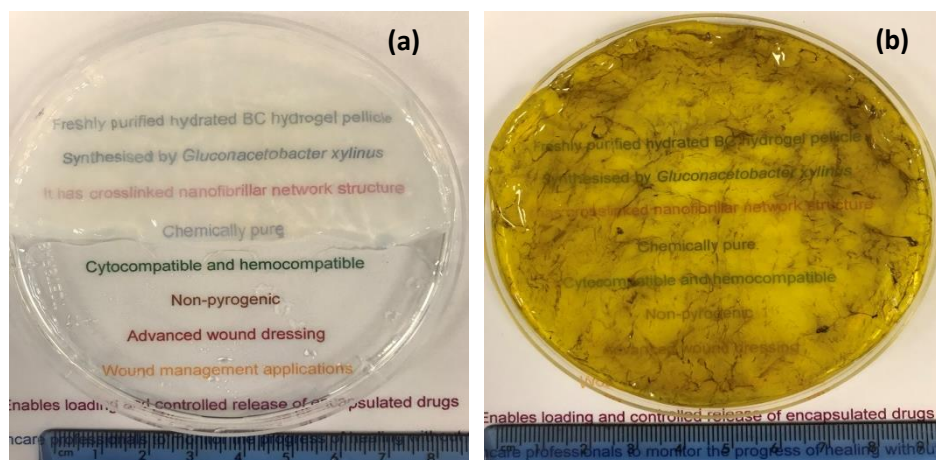


Figure. 6. Photomicrographs with the visual appearance of (a) BC loaded with PBS (b) cAgNP-loaded BC hydrogel pellicle.

■ CONCLUSION

The development of advanced polymeric materials requires precise evaluation of structure, properties and behaviour to avoid potential failures of the commercial products manufactured from them. The current study demonstrates the production, physicochemical and *in vitro* characterisation of cAgNP-loaded BC hydrogels. It also increases efficiency and minimizes the potential failure of precisely structured biomaterials before, during and after specific applications. The results confirmed that cAgNPs were successfully synthesised, following the green chemistry approach using CUR:HP β CD and loaded in BC to produce hydrogels with a potential wound dressing application. These hydrogels demonstrated broad-spectrum antimicrobial activity along with antioxidant properties. Moreover, the hydrogels showed cytocompatibility with the tested cell lines. The high moisture content and the good level of transparency further advocate their potential application in the management of chronic wounds with high microbial bioburden.

1
2
3
4
5
6
7
8
9
10
11
12
13
14
15
16
17
18
19
20
21
22
23
24
25

▪ **AUTHOR INFORMATION**

26
27

Corresponding authors

28
29
30
31
32
33
34
35
36
37
38
39
40
41

*Abhishek Gupta, Email: a.gupta@wlv.ac.uk

*Iza Radecka, Email: I.Radecka@wlv.ac.uk

*Marek Kowalczyk, Email: marek.kowalczyk@cmpw-pan.edu.pl

42
43
44
45
46
47
48
49
50
51
52
53
54
55
56
57
58
59
60

▪ **ACKNOWLEDGEMENT**

The authors would like to thank Professor Wang Weiguang and his team for their kind assistance. Abhishek Gupta would like to thanks the School of Pharmacy at the University of Wolverhampton for the support towards his PhD research. This paper is partly supported by European Union's Horizon 2020 research and innovation programme under the Marie Skłodowska-Curie grant agreement No 872152, project GREEN-MAP.

▪ **CONFLICT OF INTEREST**

The authors confirm no conflict of interest. The authors alone are responsible for the content and writing of the article.

▪ REFERENCES

- (1) James, G. A.; Swogger, E.; Wolcott, R.; Pulcini, E. d.; Secor, P.; Sestrich, J.; Costerton, J. W.; Stewart, P. S. Biofilms in chronic wounds *Wound Repair and Regeneration* **2008**, *16*, 37-44.
- (2) Duckworth, P. F.; Rowlands, R. S.; Barbour, M. E.; Maddocks, S. E. A novel flow-system to establish experimental biofilms for modelling chronic wound infection and testing the efficacy of wound dressings *Microbiol. Res.* **2018**, *215*, 141-147.
- (3) Bou Haidar, N.; Marais, S.; Dé, E.; Schaumann, A.; Barreau, M.; Feuilloley, M. G. J.; Duncan, A. C. Chronic wound healing: A specific antibiofilm protein-asymmetric release system *Mater. Sci. Eng. C.* **2020**, *106*, 110130.
- (4) Xia, G.; Zhai, D.; Sun, Y.; Hou, L.; Guo, X.; Wang, L.; Wang, F.; Li, Z. Preparation of a novel asymmetric wetttable chitosan-based sponge and its role in promoting chronic wound healing *Carbohydr. Polym.* **2020**, *227*, 115296.
- (5) Wu, Y.; Cheng, N.; Cheng, C. Biofilms in Chronic Wounds: Pathogenesis and Diagnosis *Trends Biotechnol.* **2019**, *37*, 505-517.
- (6) Williams, H.; Campbell, L.; Crompton, R. A.; Singh, G.; McHugh, B. J.; Davidson, D. J.; McBain, A. J.; Cruickshank, S. M.; Hardman, M. J. Microbial Host Interactions and Impaired Wound Healing in Mice and Humans: Defining a Role for BD14 and NOD2 *J. Invest Dermatol.* **2018**, *138*, 2264-2274.
- (7) Benjamin A. Lipsky; Kenneth J. Holroyd; Michael Zasloff Topical versus Systemic Antimicrobial Therapy for Treating Mildly Infected Diabetic Foot Ulcers: A Randomized, Controlled, Double-Blinded, Multicenter Trial of Pexiganan Cream *Clin. Infect. Dis.* **2008**, *47*, 1537-1545.
- (8) Namviriyachote, N.; Lipipun, V.; Akkhawattanangkul, Y.; Charoonrut, P.; Ritthidej, G. C. Development of polyurethane foam dressing containing silver and asiaticoside for healing of dermal wound *Asian J. Pharm. Sci.* **2019**, *14*, 63-77.
- (9) Winter, G. D. Formation of the Scab and the Rate of Epithelization of Superficial Wounds in the Skin of the Young Domestic Pig *Nature* **1962**, *193*, 293-294.
- (10) Xue, H.; Hu, L.; Xiong, Y.; Zhu, X.; Wei, C.; Cao, F.; Zhou, W.; Sun, Y.; Endo, Y.; Liu, M.; Liu, G.; Liu, Y.; Liu, J.; Abududilibaier, A.; Chen, L.; Yan, C.; Mi, B. Quaternized chitosan-Matrigel-polyacrylamide hydrogels as wound dressing for wound repair and regeneration *Carbohydr. Polym.* **2019**, *226*, 115302.
- (11) Tao, G.; Wang, Y.; Cai, R.; Chang, H.; Song, K.; Zuo, H.; Zhao, P.; Xia, Q.; He, H. Design and performance of sericin/poly(vinyl alcohol) hydrogel as a drug delivery carrier for potential wound dressing application *Mater. Sci. Eng. C.* **2019**, *101*, 341-351.
- (12) Koehler, J.; Brandl, F.P.; Goepferich, A.M. Hydrogel wound dressings for bioactive treatment of acute and chronic wounds. *Eur. Polym. J.* **2018**;100, 1-11.

- 1
2
3 (13) Gupta, A.; Kowalczyk, M.; Heaselgrave, W.; Britland, S. T.; Martin, C.; Radecka, I.
4 The production and application of hydrogels for wound management: A review *Eur.*
5 *Polym. J.* **2019**, *111*, 134-151.
6
7 (14) Costa, A. F. S.; Almeida, F. C. G.; Vinhas, G. M.; Sarubbo, L. A. Production of
8 Bacterial Cellulose by *Gluconacetobacter hansenii* Using Corn Steep Liquor As
9 Nutrient Sources *Front. Microbiol.* **2017**, *8*, 2027.
10
11 (15) Jiji, S.; Udhayakumar, S.; Rose, C.; Muralidharan, C.; Kadirvelu, K. Thymol enriched
12 bacterial cellulose hydrogel as effective material for third degree burn wound
13 repair *Int. J. Biol. Macromol.* **2019**, *122*, 452-460.
14
15 (16) Wichai, S.; Chuysinuan, P.; Chairwut, S.; Ekabutr, P.; Supaphol, P. Development of
16 bacterial cellulose/alginate/chitosan composites incorporating copper (II) sulfate as an
17 antibacterial wound dressing *J. Drug Delivery Sci. Technol.* **2019**, *51*, 662-671.
18
19 (17) Faisul Aris, F. A.; Ain Mohd Fauzi, Fatin Nur; Yenn, T. W.; Syed Abdullah, S. S.
20 Interaction of silver sulfadiazine with bacterial cellulose via *ex-situ* modification
21 method as an alternative diabetic wound healing *Biocatal. Agric. Biotechnol.* **2019**, *21*,
22 101332.
23
24 (18) Khosravi, K.; Koller, M.; Mortazavian, A.M. Bacterial nanocellulose: biosynthesis and
25 medical application *Biointerface Res. Appl. Chem.* **2016**, *6*, 1511-1516.
26
27 (19) Abeer, M.M.; Mohd, Amin.; Mohd, Cairul. Iqbal.; Martin, C. A review of bacterial
28 cellulose-based drug delivery systems: their biochemistry, current approaches and
29 future prospects. *J. Pharm. Pharmacol.* **2014**, *66*, 1047-1061.
30
31 (20) Gupta, A.; Low, W. L.; Britland, S. T.; Radecka, I.; Martin, C. Physicochemical
32 characterisation of biosynthetic bacterial cellulose as a potential wound dressing
33 material *British J. Pharm.* **2018**, *2*, S37-S38.
34
35 (21) Zmejkoski, D.; Spasojević, D.; Orlovska, I.; Kozyrovska, N.; Soković, M.; Glamočlija,
36 J.; Dmitrović, S.; Matović, B.; Tasić, N.; Maksimović, V.; Sosnin, M.; Radotić, K.
37 Bacterial cellulose-lignin composite hydrogel as a promising agent in chronic wound
38 healing *Int. J. Biol. Macromol.* **2018**, *118*, 494-503.
39
40 (22) Gupta, A.; Keddie, D. J.; Kannappan, V.; Gibson, H.; Khalil, I. R.; Kowalczyk, M.;
41 Martin, C.; Shuai, X.; Radecka, I. Production and characterisation of bacterial
42 cellulose hydrogels loaded with curcumin encapsulated in cyclodextrins as wound
43 dressings *Eur. Polym. J.* **2019**, *118*, 437-450.
44
45 (23) Kowalczyk, MM. Forensic Engineering of Advanced Polymeric Materials. *Mathews J.*
46 *Forensic Research* **2017**; *1*, e001.
47
48 (24) Kean, R. and Ramage, G. Combined Antifungal Resistance and Biofilm Tolerance:
49 the Global Threat of *Candida auris*. *mSphere* **2019**, *4*, e00458-19.
50
51 (25) Ciric, L. *Candida auris*: The new superbug on the block. *BBC*. [online] Available at:
52 <https://www.bbc.co.uk/news/health-49170866> **2019**.
53
54
55
56
57
58
59
60

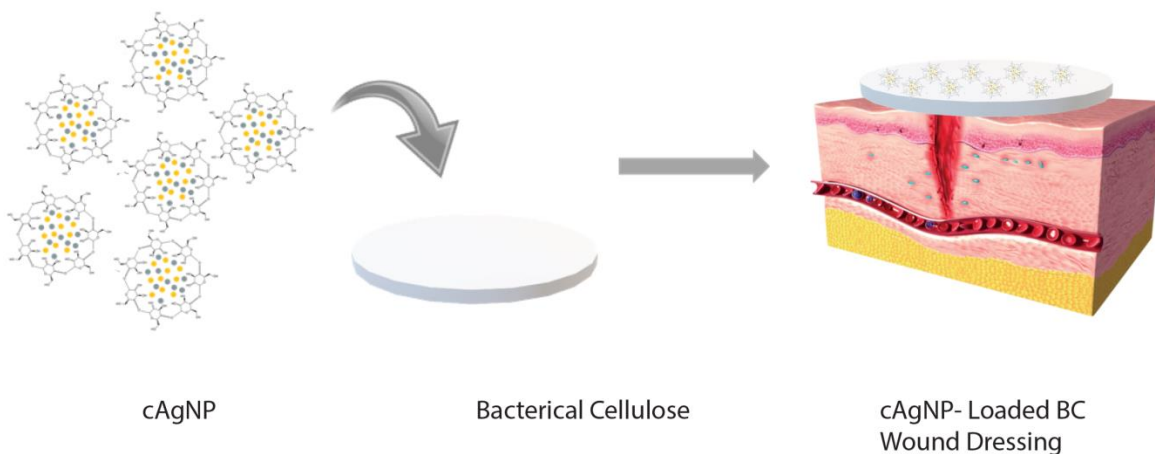
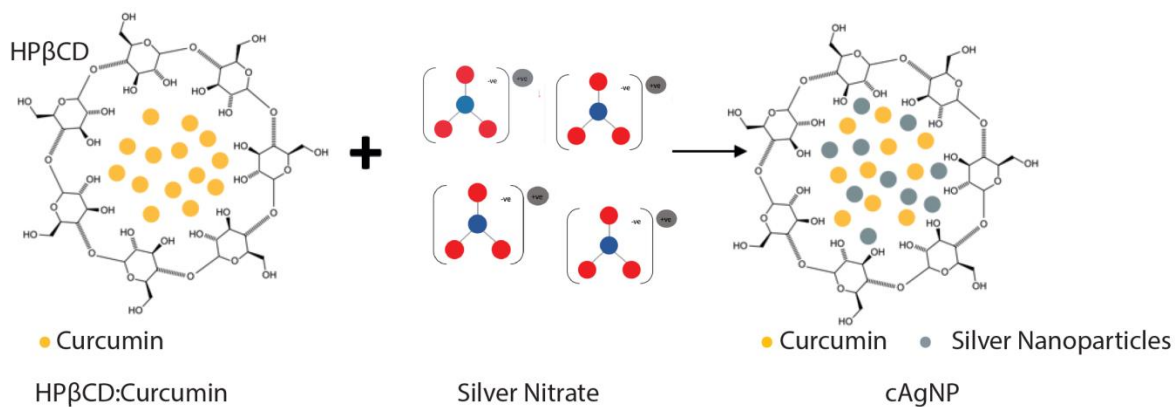
- 1
2
3 (26) Speare-Cole, R. *Candida auris*: Eight Britons who died in UK hospitals were infected
4 with Japanese super-fungus. *Evening Standard*. [online] Available at:
5 [https://www.standard.co.uk/news/uk/eight-britons-who-died-in-hospital-were-](https://www.standard.co.uk/news/uk/eight-britons-who-died-in-hospital-were-infected-with-japanese-superfungus-a4128901.html)
6 [infected-with-japanese-superfungus-a4128901.html](https://www.standard.co.uk/news/uk/eight-britons-who-died-in-hospital-were-infected-with-japanese-superfungus-a4128901.html) **2019**.
7
8 (27) Osei Sekyere, J. *Candida auris*: A systematic review and meta-analysis of current
9 updates on an emerging multidrug-resistant pathogen. *MicrobiologyOpen* **2018**, *1*,
10 e00578.
11
12 (28) Lockhart, S. *Candida auris* and multidrug resistance: Defining the new
13 normal. *Fungal Genet. Biol.* **2019**, *131*, 103243.
14
15 (29) Vallabhaneni, S., Jackson, B. and Chiller, T. *Candida auris*: An Emerging
16 Antimicrobial Resistance Threat. *Ann. Intern. Med.* **2019**, *171*, 432-433.
17
18 (30) Arikan-Akdagli, S., Ghannoum, M. and Meis, J. Antifungal Resistance: Specific Focus
19 on Multidrug Resistance in *Candida auris* and Secondary Azole Resistance in
20 *Aspergillus fumigatus*. *J. Fungi* **2018**, *4*, 129-142.
21
22 (31) Gohlar, G. and Hughes, S. How to improve antifungal stewardship. *The*
23 *Pharmaceutical J.* **2019**, *303*, 7927.
24
25 (32) Srivastava, V., Singla, R. and Dubey, A. Emerging Virulence, Drug Resistance and
26 Future Anti-fungal Drugs for *Candida* Pathogens. *Curr. Top. Med. Chem.* **2018**, *18*,
27 759-778.
28
29 (33) Gupta, A.; Low, W. L.; Radecka, I.; Britland, S. T.; Mohd Amin, Mohd Cairul Iqbal;
30 Martin, C. Characterisation and *in vitro* antimicrobial activity of biosynthetic silver-
31 loaded bacterial cellulose hydrogels *J. Microencapsul.* **2016**, *33*, 725-734.
32
33 (34) Melaiye, A.; Youngs, W. J. Silver and its application as an antimicrobial agent *Expert*
34 *Opin. Ther. Pat.* **2005**, *15*, 125-130.
35
36 (35) Brandt, O.; Mildner, M.; Egger, A. E.; Groessl, M.; Rix, U.; Posch, M.; Keppler, B.
37 K.; Strupp, C.; Mueller, B.; Stingl, G. Nanoscale silver possesses broad-spectrum
38 antimicrobial activities and exhibits fewer toxicological side effects than silver
39 sulfadiazine *Nanomedicine: Nanotechnology, Biology and Medicine* **2012**, *8*, 478-488.
40
41 (36) Parveen, A.; Kulkarni, N.; Yalagatti, M.; Abbaraju, V.; Deshpande, R. In vivo efficacy
42 of biocompatible silver nanoparticles cream for empirical wound healing *J. Tissue*
43 *Viability* **2018**, *27*, 257-261.
44
45 (37) Ravindran, J.; Arumugasamy, V.; Baskaran, A. Wound healing effect of silver
46 nanoparticles from *Tridax procumbens* leaf extracts on *Pangasius*
47 hypophthalmus *Wound Medicine* **2019**, *27*, 100170.
48
49 (38) Ahsan, A.; Farooq, M. A. Therapeutic potential of green synthesized silver
50 nanoparticles loaded PVA hydrogel patches for wound healing *J. Drug Delivery Sci.*
51 *Technol.* **2019**, *54*, 101308.
52
53
54
55
56
57
58
59
60

- 1
2
3 (39) Keshari, A. K.; Srivastava, R.; Singh, P.; Yadav, V. B.; Nath, G. Antioxidant and
4 antibacterial activity of silver nanoparticles synthesized by *Cestrum nocturnum* J.
5 *Ayurveda and Integrative Medicine* **2018**, 1-8.
6
7 (40) Alsammarraie, F. K.; Wang, W.; Zhou, P.; Mustapha, A.; Lin, M. Green synthesis of
8 silver nanoparticles using turmeric extracts and investigation of their antibacterial
9 activities *Colloids Surf., B* **2018**, 171, 398-405.
10
11 (41) Hemmati, S.; Rashtiani, A.; Zangeneh, A.; Zangeneh, M. M.; Mohammadi, P.; Veisi,
12 H. Green synthesis and characterization of silver nanoparticles using Fritillaria flower
13 extract and their antibacterial activity against some human
14 pathogens *Polyhedron* **2019**, 158, 8-14.
15
16 (42) Akbik, D.; Ghadiri, M.; Chrzanowski, W.; Rohanzadeh, R. Curcumin as a wound
17 healing agent *Life Sci.* **2014**, 116, 1-7.
18
19 (43) Song, Z.; Wu, Y.; Wang, H.; Han, H. Synergistic antibacterial effects of curcumin
20 modified silver nanoparticles through ROS-mediated pathways *Mater. Sci. Eng.*
21 *C.* **2019**, 99, 255-263.
22
23 (44) Pandit, R.; Gaikwad, S.; Agarkar, G.; Gade, A.; Rai, M. Curcumin nanoparticles:
24 physico-chemical fabrication and its *in vitro* efficacy against human pathogens *3*
25 *Biotech* **2015**, 5, 991-997.
26
27 (45) Abdulwahab, F.; Henari, F. Z.; Cassidy, S.; Winser, K. Synthesis of Au, Ag, Curcumin
28 Au/Ag, and Au-Ag Nanoparticles and Their Nonlinear Refractive Index Properties *J.*
29 *Nanomater.* **2016**, 2016, 5356404, 1-7.
30
31 (46) Yang, X. X.; Li, C. M.; Huang, C. Z. Curcumin modified silver nanoparticles for
32 highly efficient inhibition of respiratory syncytial virus infection *Nanoscale* **2016**, 8,
33 3040-3048.
34
35 (47) Murugesan, K.; Koroth, J.; Srinivasan, P. P.; Singh, A.; Mukundan, S.; Karki, S. S.;
36 Choudhary, B.; Gupta, C. M. Effects of green synthesised silver nanoparticles (ST06-
37 AgNPs) using curcumin derivative (ST06) on human cervical cancer cells (HeLa) in
38 vitro and EAC tumor bearing mice models *Int. J. Nanomed.* **2019**, 14, 5257-5270.
39
40 (48) Khan, M. J.; Shameli, K.; Sazili, A. Q.; Selamat, J.; Kumari, S. Rapid Green Synthesis
41 and Characterization of Silver Nanoparticles Arbitrated by Curcumin in an Alkaline
42 Medium *Molecules (Basel, Switzerland)* **2019**, 24, 719.
43
44 (49) Lyu, Y.; Yu, M.; Liu, Q.; Zhang, Q.; Liu, Z.; Tian, Y.; Li, D.; Changdao, M. Synthesis
45 of silver nanoparticles using oxidized amylose and combination with curcumin for
46 enhanced antibacterial activity *Carbohydr. Polym.* **2019**, 115573.
47
48 (50) Shameli, K.; Ahmad, M. B.; Zamanian, A.; Sangpour, P.; Shabanzadeh, P.; Abdollahi,
49 Y.; Zargar, M. Green biosynthesis of silver nanoparticles using *Curcuma longa* tuber
50 powder *Int. J. Nanomed.* **2012**, 7, 5603-5610.
51
52
53
54
55
56
57
58
59
60

- 1
2
3 (51) Hestrin, S.; Schramm, M. Synthesis of cellulose by *Acetobacter xylinum*. II.
4 Preparation of freeze-dried cells capable of polymerizing glucose to cellulose
5 *Biochem. J.* **1954**, *58*, 345.
6
7 (52) Liu, D.; Cao, Y.; Qu, R.; Gao, G.; Chen, S.; Zhang, Y.; Wu, M.; Ma, T.; Li, G.;
8 Production of bacterial cellulose hydrogels with tailored crystallinity from
9 *Enterobacter* sp. FY-07 by the controlled expression of colanic acid synthetic genes.
10 *Carbohydr. Polym.* **2019**, *207*, 563-570.
11
12 (53) Sathishkumar, M.; Sneha, K.; Yun, Y. Immobilization of silver nanoparticles
13 synthesized using *Curcuma longa* tuber powder and extract on cotton cloth for
14 bactericidal activity *Bioresour. Technol.* **2010**, *101*, 7958-7965.
15
16 (54) Jalili, Tabaii M.; Emtiazi, G. Transparent nontoxic antibacterial wound dressing based
17 on silver nano particle/bacterial cellulose nano composite synthesized in the presence
18 of tripolyphosphate. *J. Drug Delivery Sci. Technol.* **2018**, *44*, 244-253.
19
20 (55) Srivatsan, K. V.; Duraipandy, N.; Begum, S.; Lakra, R.; Ramamurthy, U.; Korrapati,
21 P. S.; Kiran, M. S. Effect of curcumin caged silver nanoparticle on collagen
22 stabilization for biomedical applications *Int. J. Biol. Macromol.* **2015**, *75*, 306-315.
23
24 (56) Wu, J.; Zheng, Y.; Song, W.; Luan, J.; Wen, X.; Wu, Z.; Chen, X.; Wang, Q.; Guo, S.
25 *In situ* synthesis of silver-nanoparticles/bacterial cellulose composites for slow-
26 released antimicrobial wound dressing *Carbohydr. Polym.* **2014**, *102*, 762-771.
27
28 (57) Portela, R.; Leal, C. R.; Almeida, P. L.; Sobral, R. G. Bacterial cellulose: a versatile
29 biopolymer for wound dressing applications *Microb. Biotechnol.* **2019**, *12*, 586-610.
30
31 (58) Khalid, A.; Ullah, H.; Ul-Islam, M.; Khan, R.; Khan, S.; Ahmad, F.; Khan, T.; Wahid,
32 F. Bacterial cellulose-TiO₂ nanocomposites promote healing and tissue regeneration
33 in burn mice model *RSC Adv* **2017**, *7*, 47662-47668.
34
35 (59) Pértile, R. A. N.; Moreira, S.; Gil da Costa, Rui M; Correia, A.; Guãrdao, L.; Gartner,
36 F.; Vilanova, M.; Gama, M. Bacterial Cellulose: Long-Term Biocompatibility
37 Studies *J. Biomater. Sci., Polym. Ed.* **2012**, *23*, 1339-1354.
38
39 (60) Lee, K.; Buldum, G.; Mantalaris, A.; Bismarck, A. More Than Meets the Eye in
40 Bacterial Cellulose: Biosynthesis, Bioprocessing, and Applications in Advanced Fiber
41 Composites *Macromol. Biosci.* **2014**, *14*, 10-32.
42
43 (61) Lopes, T. D.; Riegel-Vidotti, I. C.; Grein, A.; Tischer, C. A.; Faria-Tischer, Paula
44 Cristina de Sousa Bacterial cellulose and hyaluronic acid hybrid membranes:
45 Production and characterization *Int. J. Biol. Macromol.* **2014**, *67*, 401-408.
46
47 (62) Moniri, M.; Boroumand Moghaddam, A.; Azizi, S.; Abdul Rahim, R.; Bin Ariff, A.;
48 Zuhainis Saad, W.; Navaderi, M.; Mohamad, R. Production and Status of Bacterial
49 Cellulose in Biomedical Engineering *Nanomaterials* **2017**, *7*, 257.
50
51 (63) Andrade, F. K.; Silva, J. P.; Carvalho, M.; Castanheira, E. M. S.; Soares, R.; Gama, M.
52 Studies on the hemocompatibility of bacterial cellulose *J. Biomed. Mater. Res., Part*
53 *A* **2011**, *98A*, 554-566.
54
55
56
57
58
59
60

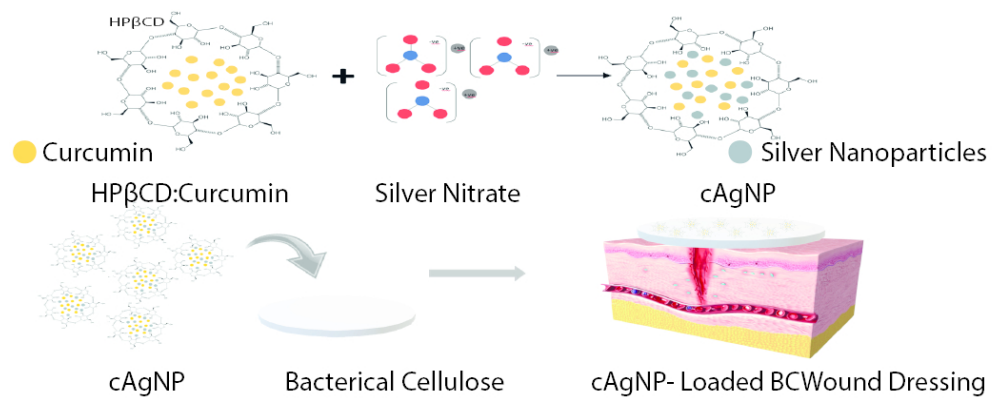
- 1
2
3 (64) Leitão, A. F.; Gupta, S.; Silva, J. P.; Reviakine, I.; Gama, M. Hemocompatibility study
4 of a bacterial cellulose/polyvinyl alcohol nanocomposite *Colloids Surf., B* **2013**, *111*,
5 493-502.
6
7 (65) ASTM F756-17. Standard Practice for Assessment of Hemolytic Properties of
8 Materials. 2017.
9
10 (66) Nagoba, B.; Davane, M. Studies on wound healing potential of topical herbal
11 formulations- do we need to strengthen study protocol? *J. Ayurveda and Integrative*
12 *Medicine* **2019**, *10*, 316-318.
13
14 (67) Guzman, M.; Dille, J.; Godet, S. Synthesis and antibacterial activity of silver
15 nanoparticles against gram-positive and gram-negative bacteria *Nanomedicine:*
16 *Nanotechnology, Biology and Medicine* **2012**, *8*, 37-45.
17
18 (68) Khatoon, U., Rao, G., Mohan, M., Ramanaviciene, A. and Ramanavicius, A.
19 Comparative study of antifungal activity of silver and gold nanoparticles synthesized
20 by facile chemical approach. *J. Environ. Chem. Eng.* **2018**, *6*, 5837-5844.
21
22 (69) Song, H.Y., Ko, K.K., Oh, I.H. and Lee, B.T.. Fabrication of silver nanoparticles and
23 their antimicrobial mechanisms. *Eur. Cells Mater.* **2006**, *11*, 58-59.
24
25 (70) Cano Sanchez, M.; Lancel, S.; Boulanger, E.; Neviere, R. Targeting Oxidative Stress
26 and Mitochondrial Dysfunction in the Treatment of Impaired Wound Healing: A
27 Systematic Review *Antioxidants (Basel, Switzerland)* **2018**, *7*, 98.
28
29 (71) Ahmed, O. M.; Mohamed, T.; Moustafa, H.; Hamdy, H.; Ahmed, R. R.; Aboud, E.
30 Quercetin and low level laser therapy promote wound healing process in diabetic rats
31 via structural reorganization and modulatory effects on inflammation and oxidative
32 stress *Biomed. Pharmacother.* **2018**, *101*, 58-73.
33
34 (72) Flanagan, M. Wound measurement: can it help us to monitor progression to healing?
35 *J. Wound Care.* **2003**, *12*, 189-194.
36
37 (73) Kenworthy, P.; Phillips, M.; Grisbrook, T. L.; Gibson, W.; Wood, F. M.; Edgar, D. W.
38 Monitoring wound healing in minor burns—A novel approach *Burns* **2018**, *44*, 70-76.
39
40 (74) Malone, M.; Schwarzer, S.; Walsh, A.; Xuan, W.; Al Gannass, A.; Dickson, H. G.;
41 Bowling, F. L. Monitoring wound progression to healing in diabetic foot ulcers using
42 three-dimensional wound imaging *J. Diabetes Complications.* **2019**, 107471.
43
44
45
46
47
48
49
50
51
52
53
54
55
56
57
58
59
60

For Table of Contents Only



Synthesis of silver nanoparticles using curcumin-cyclodextrins loaded into bacterial cellulose based hydrogels for wound dressing applications

Abhishek Gupta^{*}, Sophie M Briffa, Sam Swingler, Hazel Gibson, Vinodh Kannappan, Grazyna Adamus, Marek Kowalczyk^{*}, Claire Martin⁶, Iza Radecka^{*}



For Table of Contents Only